

An Enhanced Mechanism to Detect Distorted Fingerprints

Sravanvardhan Rao Souda

Assistant Professor,

Ellenki College of Engineering & Technology,
Hyderabad.

Jangam Ravi

Assistant Professor,

Avanthi's Scientific Technological & Research
Academy, Hyderabad.

Abstract:

Elastic distortion of fingerprints is one of the major causes for false non-match. While this problem affects all fingerprint recognition applications, it is especially dangerous in negative recognition applications, such as watch list and deduplication applications. In such applications, malicious users may purposely distort their fingerprints to evade identification. In this paper, we proposed novel algorithms to detect and rectify skin distortion based on a single fingerprint image. Distortion detection is viewed as a two-class classification problem, for which the registered ridge orientation map and period map of a fingerprint are used as the feature vector and a SVM classifier is trained to perform the classification task. Distortion rectification (or equivalently distortion field estimation) is viewed as a regression problem, where the input is a distorted fingerprint and the output is the distortion field.

To solve this problem, a database (called reference database) of various distorted reference fingerprints and corresponding distortion fields is built in the offline stage, and then in the online stage, the nearest neighbor of the input fingerprint is found in the reference database and the corresponding distortion field is used to transform the input fingerprint into a normal one. Promising results have been obtained on three databases containing many distorted fingerprints, namely FVC2004 DB1, Tsinghua Distorted Fingerprint database, and the NIST SD27 latent fingerprint database.

Index Terms:

Fingerprint, distortion, registration, nearest neighbor regression, PCA.

1 INTRODUCTION:

ALTHOUGH automatic fingerprint recognition technologies have rapidly advanced during the last forty years, there still exists several challenging research problems, for example, recognizing low quality fingerprints [2]. Fingerprint matcher is very sensitive to image quality as observed in the FVC2006 [3], where the matching accuracy of the same algorithm varies significantly among different datasets due to variation in image quality. The difference between the accuracies of plain, rolled and latent fingerprint matching is even larger as observed in technology evaluations conducted by the NIST [4]. The consequence of low quality fingerprints depends on the type of the fingerprint recognition system. A fingerprint recognition system can be classified as either a positive or negative system. In a positive recognition system, such as physical access control systems, the user is supposed to be cooperative and wishes to be identified.

In a negative recognition system, such as identifying persons in watch lists and detecting multiple enrollment under different names, the user of interest (e.g., criminals) is supposed to be uncooperative and does not wish to be identified. In a positive recognition system, low quality will lead to false reject of legitimate users and thus bring inconvenience. The consequence of low quality for a negative recognition system, however, is much more serious, since malicious users may purposely reduce fingerprint quality to prevent fingerprint system from finding the true identity [6]. In fact, law enforcement officials have encountered a number of cases where criminals attempted to avoid identification by damaging or surgically altering their fingerprints [7].

Hence it is especially important for negative fingerprint recognition systems to detect low quality fingerprints and improve their quality so that the fingerprint system is not compromised by malicious users. Degradation of finger-print quality can be photometric or geometrical. Photometric degradation can be caused by non-ideal skin conditions, dirty sensor surface, and complex image background (especially in latent fingerprints). Geometrical degradation is mainly caused by skin distortion. Photometric degradation has been widely studied and a number of quality evaluation algorithms [8], [9], [10] and enhancement algorithms [11], [12], [13], [14], [15] have been proposed. On the contrary, geometrical degradation due to skin distortion has not yet received sufficient attention, despite of the importance of this problem. This is the problem this paper attempts to address.

Note that, for a negative fingerprint recognition system, its security level is as weak as the weakest point. Thus it is urgent to develop distorted fingerprint (DF) detection and rectification algorithms to fill the hole. Elastic distortion is introduced due to the inherent flexibility of fingertips, contact-based fingerprint acquisition procedure, and a purposely lateral force or torque, etc. Skin distortion increases the intra-class variations (difference among fingerprints from the same finger) and thus leads to false non-matches due to limited capability of existing fingerprint matchers in recognizing severely distorted fingerprints. In Fig. 1, the left two are normal fingerprints, while

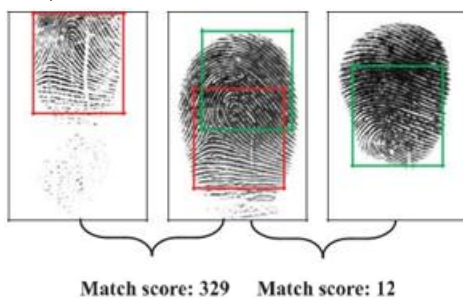


Fig. 1. Three impressions of the same finger from FVC2004 DB1.

The left two are normal fingerprints, while the right one contains severe distortion. The match score between the left two according to VeriFinger 6.2 SDK [5], is much higher than the match score between the right two. This huge difference is due to distortion rather than overlapping area. As shown by red and green rectangles, the overlapping area is similar in two cases. the right one contains severe distortion. According to Veri-Finger 6.2 SDK [5], the match score between the left two is much higher than the match score between the right two. This huge difference is due to distortion rather than over-lapping area. While it is possible to make the matching algorithms tolerate large skin distortion, this will lead to more false matches and slow down matching speed. In this paper, novel algorithms are proposed to deal with the fingerprint distortion problem. See Fig. 2 for the flowchart of the proposed system. Given an input finger-print, distortion detection is performed first.

If it is determined to be distorted, distortion rectification is performed to transform the input fingerprint into a normal one. A distorted fingerprint is analogous to a face with expression, which affects the matching accuracy of face recognition systems. Rectifying a distorted fingerprint into a normal fingerprint is analogous to transforming a face with expression into a neutral face, which can improve face recognition performance. In this paper, distortion detection is viewed as a two-class classification problem, for which the registered ridge orientation map and period map of a fingerprint are used as the feature vector and a SVM classifier is trained to perform the classification task. Distortion rectification (or equivalently distortion field estimation) is viewed as a regression problem, where the input is a distorted fingerprint and the output is the distortion field. To solve this problem, a database of various distorted reference fingerprints and corresponding distortion fields is built in the offline stage, and then in the online stage, the nearest neighbor of the input fingerprint is found in the database of distorted reference fingerprints and the corresponding distortion field is used to rectify the input fingerprint.

An important property of the proposed system is that it does not require any changes to existing fingerprint sensors and fingerprint acquisition procedures. Such property is important for convenient incorporation into existing fingerprint recognition systems. The proposed system has been evaluated on three data-bases, FVC2004 DB1 whose images are markedly affected by distortion, Tsinghua distorted fingerprint database which contains 320 distorted fingerprint video files, and NIST SD27 latent fingerprint database. Experimental results demonstrate that the proposed algorithms can improve the matching accuracy of distorted fingerprints evidently. The remainder of this paper is organized as follows. In Section 2, we review the related work. In Section 3, we explain how to detect distorted fingerprints. In Section 4, we present the distorted fingerprint rectification algorithm in details. In Section 5, we give the experiment results. In Section 6, we summarize the paper and discuss the future research directions.

2 RELATED WORK:

Due to the vital importance of recognizing distorted fingerprints, researchers have proposed a number of methods which can be coarsely classified into four categories.

2.1 Distortion Detection Based on Special Hardware:

It is desirable to automatically detect distortion during fingerprint acquisition so that severely distorted fingerprints can be rejected. Several researchers have proposed to detect improper force using specially designed hard-ware [16], [17], [18]. Bolle et al. [16] proposed to detect excessive force and torque exerted by using a force sensor. They showed that controlled fingerprint acquisition leads to improved matching performance [17]. Fujii [18] proposed to detect distortion by detecting deformation of a transparent film attached to the sensor surface. Dorai et al. [19] proposed to detect distortion by analyzing the motion in video of fingerprint.

However, the above methods have the following limitations: (i) they require special force sensors or fingerprint sensors with video capturing capability; (ii) they cannot detect distorted fingerprint images in existing fingerprint databases; and (iii) they cannot detect fingerprints distorted before pressing on the sensor.

2.2 Distortion-Tolerant Matching:

The most popular way to handle distortion is to make the fingerprint matcher tolerant to distortion [20], [21], [22], [23], [24], [25]. In other words, they deal with distortion on a case by case basis, i.e., for every pair of fingerprints to be

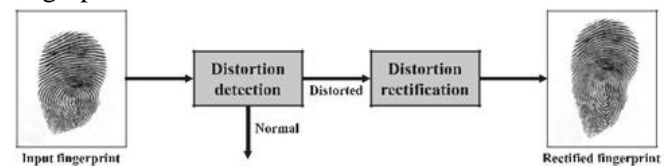


Fig. 2. Flowchart of the proposed distortion detection and rectification system.

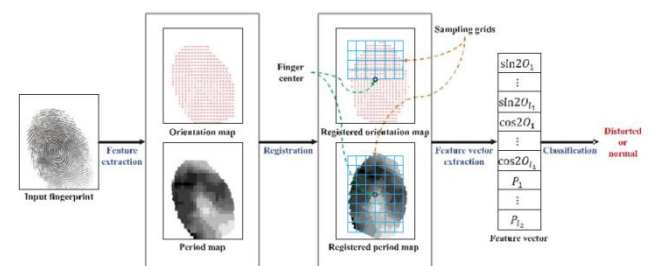


Fig. 3. Flowchart of fingerprint distortion detection.

O_i represents ridge orientation at the i th sampling grid of registered orientation map, while P_j represents ridge period at the j th sampling grid of registered period map. l_1 and l_2 represent the number of sampling points in registered orientation map and registered period map, respectively. compared. For the most widely used minutiae-based fingerprint matching method, the following three types of strategies have been adopted to handle distortion: (i) assume a global rigid transformation and use a tolerant box of fixed size [20] or adaptive size [21] to compensate for distortion;

(ii) explicitly model the spatial transformation by thin plate spline (TPS) model [22]; and (iii) enforce constraint on dis-tortion locally [24]. Various methods for handling distortion during matching have also been used in image-based matcher [23] or skeleton-based matcher [25]. However, allowing larger distortion in matching will inevitably result in higher false match rate. For example, if we increased the bounding zone around a minutia, many non-mated minutiae will have a chance to get paired. In addition, allowing larger distortion in matching will also slow down the matching speed.

2.3. Distortion Rectification Based on Finger-Specific Statistics:

Ross et al. [26], [27] learn the deformation pattern from a set of training images of the same finger and transform the tem-plate with the average deformation. They show this leads to higher minutiae matching accuracy. But this method has the following limitations: (i) acquir-ing multiple images of the same finger is inconvenient in some applications and existing fingerprint databases gener-ally contain only one image per finger; and (ii) even if multi-ple images per finger are available, it is not necessarily sufficient to cover various skin distortions.

2.4. Distortion Rectification Based on General Statistics:

Senior and Bolle [28] developed an interesting method to remove the distortion before matching stage. This method is based on an assumption that the ridges in a fingerprint are constantly spaced. So they deal with distortion by normalizing ridge density in the whole fingerprint into a fixed value. Since they did not have a distortion detection algorithm, they apply the distortion rectification algo-rithm to every fingerprint. Compared to the other methods reviewed above, Senior and Bolle method has the following advantages: (i) it does not require specialized hardware; (ii) it can handle a single input fingerprint image; and (iii) it does not require a set of training images of the same finger.

However, ridge density is neither fixed within a finger nor fixed across fingers. In fact, several researchers have reported improved matching accuracy due to incorporating ridge density information into minutiae matchers [29], [30]. Simply normalizing ridge density of all fingerprints will lose discriminating information in fingerprints and may improve impostor match scores. Furthermore, without any constraint on validity of orientation map, this method may generate fingerprints with fixed ridge period but strange orientation map. Compare to the first limitation, the second limitation is even more harmful, since it will reduces genu-ine match scores. These limitations were not found in [28] since the algorithm was tested only on a small database con-sisting of six fingers and finger rotation was not considered.

Our method shares the advantages of Senior and Bolle method over other methods, meanwhile overcomes some of its limitations. Our method is based on statistics learnt from real distorted fingerprints, rather than on the impractical assumption of uniform ridge period made in [28]. Distortion due to finger rotation can be handled by our method. In fact, the proposed method is able to deal with various types of distortion as long as such distortion type is contained in the training set. In addition, extensive experiments have been conducted to validate the proposed method. The current work is a significant update of our preliminary study in [1], which detects distortion based on simple hand-crafted fea-tures and has no rectification functionality.

3 FINGERPRINT DISTORTION DETECTION:

Fingerprint distortion detection can be viewed as a two-class classification problem. We used the registered ridge orientation map and period map as the feature vector, which is classified by a SVM classifier. The distortion detec-tion flowchart is shown in Fig. 3.

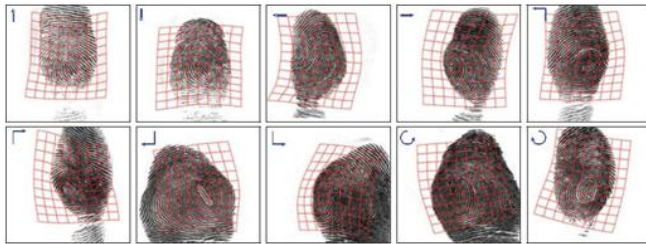


Fig. 4. Examples of 10 distortion types in Tsinghua DF database. The blue arrows represent the directions of force or torque, and red grids represent the distortion grids which are calculated from matched minutiae between the normal fingerprint and the distorted fingerprint.

3.1 Fingerprint Registration:

In order to extract meaningful feature vector, fingerprints have to be registered in a fixed coordinate system. For this task, we propose a multi-reference based fingerprint registration approach. In the following, we describe how the reference fingerprints are prepared in the offline stage, and how to register an input fingerprint in the online stage.

3.1.1 Reference Fingerprints:

In order to learn statistics of realistic fingerprint distortion, we collected a distorted fingerprint database called Tsinghua distorted fingerprint database. A FTIR fingerprint scanner with video capture functionality was used for data collection. Each participant is asked to press a finger on the scanner in a normal way, and then distort the finger by applying a lateral force or a torque and gradually increase the force. A total of 320 videos (with a frame rate of 10 FPS) were obtained from 185 different fingers. Each finger produces 10 videos and each video contains only one of ten different distortion types as shown in Fig. 4. In every video, the first frame is the normal fingerprint, and the last frame contains largest distortion. The duration of each video is around 10 seconds. For training and testing purpose, the collected database is divided into two parts with $n_{train} = \frac{1}{4} \cdot 200$ videos used as training data and $n_{test} = \frac{1}{4} \cdot 120$ videos used as testing data.

In each video, only the first frame (normal fingerprint) and the last frame (distorted fingerprint) are used for training and testing. Note that all fingerprints have a resolution of 500 ppi. We use 500 fingerprints as reference fingerprints which consist of 100 normal fingerprints from FVC2002 DB1_A, 200 pairs of normal and distorted fingerprints from the training set of Tsinghua DF database. Note that there are no common fingerprints between training and testing data. A large number of references are used in order to properly register fingerprints of various pattern types, while distorted fingerprints are also used as references in order that new distorted fingerprints can be properly registered. A reference fingerprint is registered based on its finger center and direction. For fingerprints whose core points can be correctly detected by a Poincare index based algorithm [31], the upper core point is used as the finger center. For arch fingerprints and those fingerprints whose upper core points are not correctly detected, we manually estimate the center point. Finger direction is defined to be vertical to finger joint and was manually marked for all reference fingerprints. Since the reference fingerprints were registered in the offline stage, manual intervention is acceptable. Fig. 5 shows the finger center and direction for two reference fingerprints.

3.1.2 Online Fingerprint Registration:

In the online stage, given an input fingerprint, we perform the registration w.r.t. registered reference fingerprints. Level 1 features (orientation map, singular points, period map) are extracted using traditional algorithms [11], [31]. According to whether the upper core point is detected or not, the registration approach can be classified into two cases. If the upper core point is not detected, we do a full search to find the pose information, namely solve the following optimization formula:

$$\begin{aligned} & \text{OrientDiff } \mathbf{RO} \ x; y; a; \\ & \max_{x,y} \mathbf{O} \quad u; \quad 1 \\ & \arg \min_{i, k} \mathbf{d} \quad i \mathbf{d} \quad \mathbf{P} \quad \mathbf{P} \quad 0 \quad () \end{aligned}$$

where x and y denote the translation parameters, α denotes the rotation parameter, i denotes the corresponding refer-ence fingerprint ID, \mathbf{O} is the orientation map of the input fingerprint, \mathbf{RO}_i denotes the orientation map of the i th refer-ence fingerprint, function $\text{OrientDiff}(\mathbf{O}, \mathbf{RO}_i)$ computes the differ-ence of two orientation maps at each location, k counts the number of nonzero elements, and k_0 counts the number of nonzero elements, and u_t is the threshold, which is empirically set as 10 degrees. Note that the ridge orientation map is defined on blocks of 16 16 pixels.

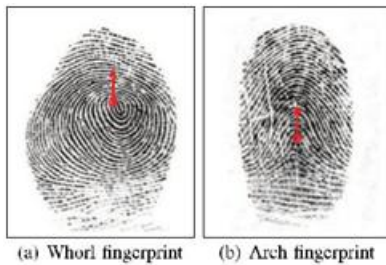


Fig. 5. The center (indicated by red circle) and direction (indicated by red arrow) of two fingerprints.

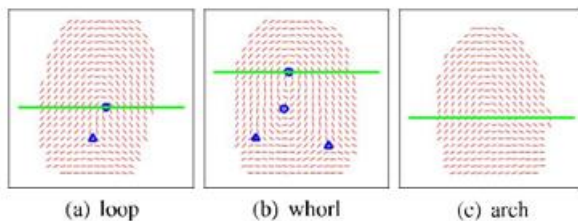


Fig. 6. Orientation maps of three patterns: (a) loop, (b) whorl, and (c) arch. A fingerprint is separated into tworegions by the green separating lines crossing the center points.

The orientation maps above the lines are similar, while orientation maps below the lines are very different. If the upper core point is detected in the input fingerprint, we align the upper core point to the center point of reference fingerprints. Namely, $\delta x; y$ is known. We find the optimal rotation parameter for Eq. (1). Finally, we register the ridge orientation map and period map of the input fingerprint to the fixed coordinate system by using the obtained pose information. The flowchart in Fig. 3 shows an example of registration.

3.2 Feature Vector Extraction:

We extract a feature vector by sampling registered orientation map and period map. The sampling grid is shown in Fig. 3, where finger center is also marked. Note that the two sampling grids are different. The sampling grid of period map covers the whole fingerprint, while the sampling grid of orientation map covers only the top part of the fingerprint. This is because the orientation maps below finger center are very diverse even within normal fingerprints. See Fig. 6 for examples. So they are not good features for distinguish distorted fingerprints from normal fingerprints. The feature vector is defined as $\frac{1}{2} \sin \delta \mathbf{2OP} \cos \delta \mathbf{2OP}$ &, where \mathbf{O} denotes the orientation vector on sampling grids, and \mathbf{P} denotes the period vector on sampling grids. Feature value at sampling points outside fingerprint region is set as 0.

3.3 Classification:

The 500 reference fingerprints that we mentioned in Section 3.1, were used as training samples. Distorted fingerprints are viewed as positive samples while normal fingerprints are viewed as negative samples. LibSVM [32] was used to train a Support Vector Classifier with quadratic polynomial kernel. All parameters used in LibSVM are default ones. Specifically, SVM type is C-SVC, g in kernel function is $1=L$ (L is the length of feature vector), and coef0 in kernel function is 0.

4 DISTORTED FINGERPRINT RECTIFICATION:

A distorted fingerprint can be thought of being generated by applying an unknown distortion field \mathbf{d} to the normal fingerprint, which is also unknown. If we can estimate the distortion field \mathbf{d} from the given distorted fingerprint, we can easily rectify it into the normal fingerprint by applying the inverse of \mathbf{d} . So we need to address a regression problem, which is quite difficult because of the high dimensionality of the distortion field (even if we use a block-wise distortion field). In this paper, a nearest neighbor regression approach is used for this task.

The proposed distorted fingerprint rectification algorithm consists of an offline stage and an online stage. In the offline stage, a database of distorted reference fingerprints is generated by transforming several normal reference fingerprints with various distortion fields sampled from the statistical model of distortion fields. In the online stage, given a distorted input fingerprint (which is detected by the algorithm described in Section 3), we retrieve its nearest neighbor in the distorted reference fingerprint database and then use the inverse of the corresponding distortion field to rectify the distorted input fingerprint. The distorted fingerprint rectification flowchart is shown in Fig. 7. In the first two sections, we describe the two steps of the offline stage: statistical modeling of distortion fields and generation of distorted reference fingerprint database. In Section 4.3, we explain how to estimate the distortion field of an input fingerprint by nearest neighbor search.

4.1 Statistical Modeling of Distortion Fields:

In order to learn statistical fingerprint distortion model, we need to know the distortion fields (or deformation fields) between paired fingerprints (the first frame and the last frame of each video) in the training set. The distortion field between a pair of fingerprints can be estimated based on the corresponding minutiae of the two fingerprints. Unfortunately, due to the severe distortion between paired fingerprints, existing minutiae matchers cannot find corresponding minutiae reliably. Thus, we extract minutiae in the first frame using VeriFinger and perform minutiae tracking in each video. Since the relative motion between adjacent frames is small, reliable minutiae correspondences between the first frame and the last frame can be found by this method. Given the matching minutiae of a pair of fingerprints, we estimate the transformation using thin plate spline model. We define a regular sampling grid on the normal fingerprint and compute the corresponding grid (called distortion grid) on the distorted fingerprint using the TPS model. Fig. 4. shows the distortion grids on 10 distorted fingerprints.

Let \mathbf{x}_i^N and \mathbf{x}_i^D denote the coordinate vectors of sampling grids of the i th pair of normal fingerprint and distortion fingerprint. The distortion field of the i th pair of fingerprints is given by

$$\mathbf{d}_i = \mathbf{x}_i^D - \mathbf{x}_i^N \quad (2)$$

Given a set of distortion fields $\mathbf{d}_i; i = 1; \dots; n_{train}$, we use PCA to get a statistical distortion model that captures the statistical variations of the training distortion fields [34], [35], [36]. Since all normal fingerprints are registered using the method in Section 3.1, the distortion fields of all training fingerprints can be viewed as feature vectors. From all n_{train} distortion field samples, a mean distortion field, $\bar{\mathbf{d}} = \frac{1}{n_{train}} \sum_{i=1}^{n_{train}} \mathbf{d}_i$, is first computed, and then a dif-

ference vector $\mathbf{d}_i - \bar{\mathbf{d}}$ for each \mathbf{d}_i is calculated to

construct an overall difference matrix D :

$$D = \begin{bmatrix} \mathbf{d}_1 - \bar{\mathbf{d}} & \dots & \mathbf{d}_{n_{train}} - \bar{\mathbf{d}} \end{bmatrix} \quad (3)$$

From this overall difference matrix, we can compute a covariance matrix

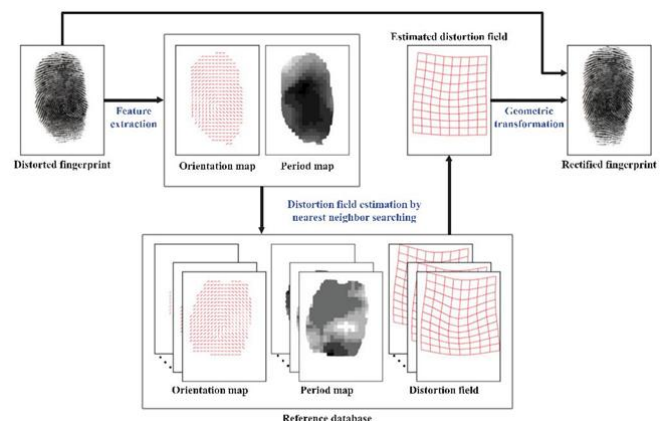


Fig. 7. Flowchart of distorted fingerprint rectification.

$$Cov(D) = \frac{1}{n_{train}} DD^T \quad (4)$$

Next, we calculate the eigenvectors $f_{i,g}$ and eigenvalues $f_{i,g}$ (sorted in decreasing order) of this covariance matrix. The eigenvalues reflect the energy distribution of the training distortion fields among eigenvectors, and the eigenvectors with the largest eigenvalues generally cover the majority of the energy within the training distortion fields. Therefore, a small number of eigenvectors, serving as basis functions, can well capture the distribution of training distortion fields. By using this distortion model, a new distortion field d can be approximated as

$$d = \sum_{i=1}^t c_i f_{i,g} \quad (5)$$

where c_i are the coefficients on the respective eigenvectors, and t is the number of selected eigenvectors. Fig. 8 shows the first two principal components as distortion grids.

4.2. Generation of Distorted Reference Fingerprint Database:

To generate the database of distorted reference fingerprints, we use $n_{ref} \approx 100$ normal fingerprints from FVC2002 DB1_A which are same to what we described in Section 3.1. Note that, these fingerprints have been registered following the procedure described in Section 3.1. The distortion fields are generated by uniformly sampling the subspace spanned by the first two principle components. For each basis, 11 points are uniformly sampled in the interval $[-2,2]$. See Fig. 9 for an example of generating distortion fields and applying such distortion fields to a reference fingerprint to generate corresponding distorted fingerprints. In Fig. 9, for visualization purpose, only one reference fingerprint (the fingerprint located at the origin of the coordinate system) is used to generate the database of distorted reference fingerprints, and for each basis, five points are sampled. In practice, multiple reference fingerprints are used to achieve better performance.

Also note

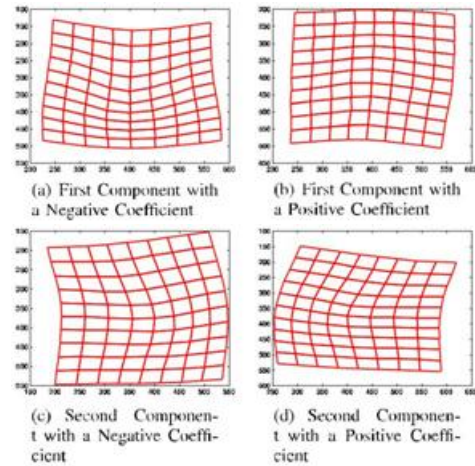


Fig. 8. First two principal components of distortion fields from the training set of Tsinghua DF database.

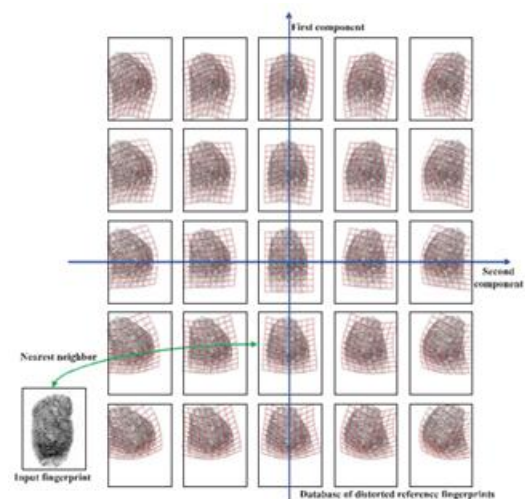


Fig. 9. Estimating the distortion field of an input fingerprint is equal to searching its nearest neighbor in the database of distorted reference fingerprints.

Here, for visualization purpose, only one reference fingerprint (the fingerprint located at the origin of the coordinate system) is used to generate the database of distorted reference fingerprints. In practice, multiple reference fingerprints are used to achieve better performance. that instead of storing the fingerprint image, we store the ridge orientation map and period map of each fingerprint in the reference database.

4.3. Distortion Field Estimation by Nearest Neighbor Search:

Distortion field estimation is equal to finding the nearest neighbor among all distorted reference fingerprints as shown in Fig. 9. The similarity is measured based on level 1 features of fingerprint, namely ridge orientation map and period map. We conjecture that distortion detection and rectification of human experts also relies on these features instead of minutiae. The similarity computation method is different depending on whether the upper core point can be detected in the input fingerprint. If the upper core point is detected, we translate the input fingerprint by aligning the upper core point to center point. Then we do a full search of u in the interval $\frac{1}{2} 30 ; 30$ & for the maximum similarity. For a specific u , the similarity between two fingerprints is computed as follows:

$$s = \frac{s_1^O}{\frac{1}{4}m} \frac{p s_2^O}{p} \frac{w_1^O s_1^O}{p} \frac{w_2^O s_2^O}{p} \frac{s_1^P}{p} \frac{p s_2^P}{m} \frac{w_1^P s_1^P}{p} \frac{w_2^P s_2^P}{p}; \quad (6)$$

where m denotes the number of blocks in the overlapping area, s_1^O and s_2^O denote the number of blocks with similar orientation above and below the center point, s_1^P and s_2^P denote the number of blocks with similar period above and below the center point, and the four weights w_1^O , w_2^O , w_1^P , w_2^P , are empirically set as 1, 0.5, 1, 1.5, respectively.

TABLE 1
Fingerprint Databases Used in This Study¹

Database	Description	Purpose
FVC2002 DB1_A	100 normal fingerprints	reference fingerprints
FVC2004 DB1	880 fingerprints	algorithm evaluation
FVC2006 DB2_A	1,580 fingerprints scaled to 500 ppi	algorithm evaluation
Tsinghua DF	320 fingerprint videos	training and algorithm evaluation
NIST SD27	258 pairs of latent & rolled fingerprints	algorithm evaluation
NIST SD14	27,000 fingerprints	background database

¹All fingerprints have a resolution of 500 ppi.

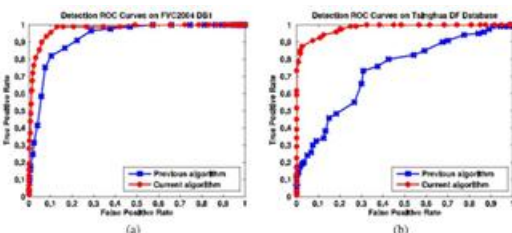


Fig. 10. The Detection ROC curves of our previous algorithm [1] and current algorithm on the (a) FVC2004 DB1 and (b) Tsinghua DF database.

Thresholds for similar orientation and similar period are empirically set 10 degrees and 1 pixel, respectively. If no upper core point is detected, we use generalized Hough transform algorithm [37], [38] to compute the similarity between two fingerprints, which is more efficient than computing Eq. (6) for all possible translation and rotation parameters.

5 EXPERIMENT:

In this section, we first evaluate the proposed distortion detection algorithm. Then, we evaluate the proposed distortion rectification algorithm by performing matching experiments on three databases. Finally, we discuss the impact of the number of reference fingerprints on distorted fingerprint rectification. Table 1 provides a summary of the databases used in this study.

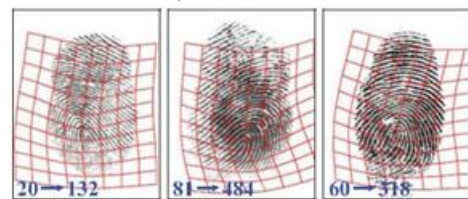


Fig. 11. Three distorted examples. Our previous algorithm [1] fails to detect their distortion, while the current algorithm can detect their distortion correctly.

The red transformation grids estimated by the proposed algorithm are overlaid on them. The blue numbers show the matching scores without/with rectification. It shows the importance of detecting them as distorted fingerprints. First two examples come from FVC2004 DB1, while the last one comes from Tsinghua DF database.

5.1. Performance of Distortion Detection:

We view distortion detection as a two-class classification problem. Distorted fingerprints are viewed as positive samples and normal fingerprints as negative samples. If a distorted fingerprint is classified as a positive sample, a true positive occurs. If a normal fingerprint is classified as a positive sample, a false positive occurs.

By changing the decision threshold, we can obtain the receiver operating characteristic (ROC) curve. Fig. 10 shows the ROC curves of the proposed algorithm and our previous algorithm [1] on FVC2004 DB1 and the test set of Tsinghua DF database. The test set of Tsinghua DF database contains 120 pairs of distorted and normal fingerprints. FVC2004 DB1 contains

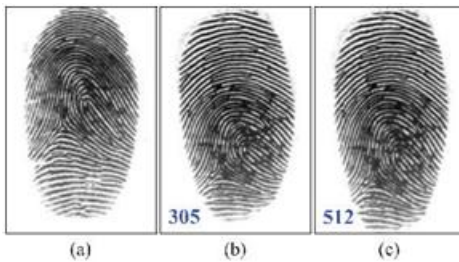


Fig. 12. An example of false negative due to slight distortion. (a) Gallery fingerprint, (b) query fingerprint, and (c) query fingerprint rectified by the proposed rectification algorithm.

Although this query fingerprint is not detected as a distorted fingerprint, due to its slight distortion, it can still be successfully matched with the gallery fingerprint by VeriFinger (the matching score is as high as 305). If we apply the rectification algorithm to the query fingerprint, its matching score with the gallery fingerprint is further improved to 512.

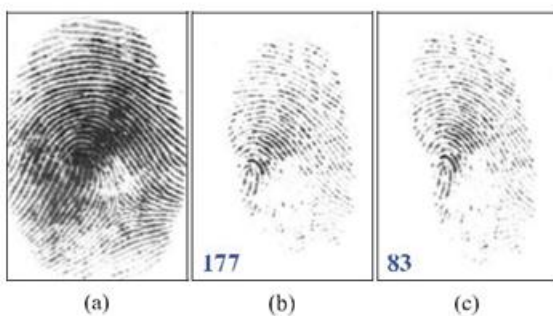


Fig. 13. An example of false positive due to low quality and small area.

(a) Gallery fingerprint, (b) query fingerprint, and (c) query fingerprint rectified by the proposed rectification algorithm. The matching scores are overlaid on the images.

791 normal fingerprints and 89 distorted fingerprints, which are found by visually examining the images. As we can see from this figure, the current algorithm performs much better. Three distorted examples in Fig. 11 further demonstrate the superior detection performance of current algorithm over our previous algorithm. Although most fingerprints can be correctly classified, there are some false negatives and false positives. False negatives are mainly because the distortion is slight. Fortunately, we found that this is not a severe problem since fingerprint matchers can successfully match slightly distorted fingerprints. Such an example is given in Fig. 12. As the query fingerprint contains slight distortion, the proposed detection algorithm fails to detect it as distorted one, but the matching score between the query fingerprint and the gallery fingerprint is 305, a very high matching score according to VeriFinger. If this query fingerprint is rectified by the proposed rectification algorithm, the matching score can be further improved to 512. False positives are mainly due to low image quality, small finger area, or non-frontal pose of finger. In such cases, there is no sufficient information for correctly aligning and classifying the fingerprint. Such an example is

TABLE 2
Statistics of Detection Error

Database	False negatives (#Error/#Total)		False positives (#Error/#Total)		
	Slight distortion	Low quality	Small area	Non-frontal pose	
FVC 2004 DB1	9/89	26/791	16/791	6/791	
Tsinghua DF	7/120	5/120	0/120	8/120	

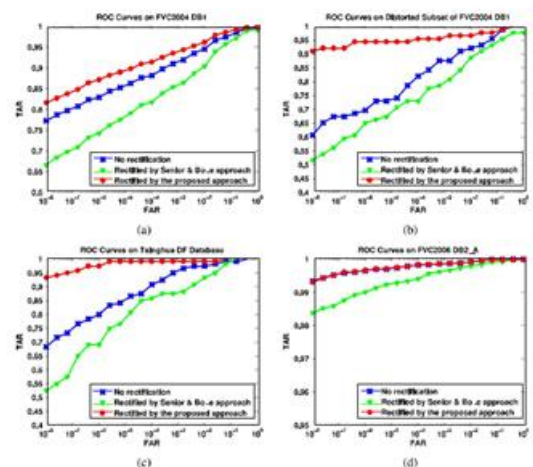


Fig. 14. The ROC curves of three fingerprint matching experiments on each of the following four databases: (a) FVC2004 DB1, (b) distorted subset

of FVC2004 DB1, (c) Tsinghua DF database, and (d) FVC2006 DB2_A.

The input images to VeriFinger in three matching experiments are original fingerprints (no rectification is performed), fingerprints rectified by Senior and Bolle approach [28], and fingerprints rectified by the proposed approach, respectively.

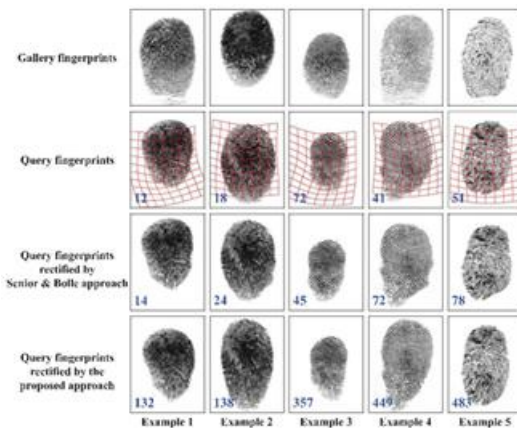


Fig. 15. Genuine match scores of original query fingerprints and query fingerprints rectified by two different approaches for five examples (left three from FVC2004 DB1, right two from Tsinghua DF database).

The red transformation grids estimated by the proposed approach are overlaid on the original query fingerprints to visualize the distortion. We can see that the distortion between query fingerprints and gallery fingerprints is greatly reduced by the proposed approach, leading to higher matching scores. shown in Fig. 13. Applying rectification to normal fingerprints may reduce matching scores. We have examined all detection errors on FVC 2004 DB1 and Tsinghua DF database and have categorized the reasons into four types. The results are shown in Table 2. Note that this classification is not exclusive and one example might be attributed to multiple reasons (such as both low quality and small area).

5.2 Performance of Distortion Rectification:

The final purpose of rectifying distorted fingerprints is to improve matching performance.

To quantitatively evaluate the contribution of the proposed rectification algorithm to the matching accuracy, we conducted three matching experiments on each of the following four databases: FVC2004 DB1, distorted subset of FVC2004 DB1, Tsinghua DF database, and FVC2006 DB2_A. VeriFinger 6.2 SDK was used as the fingerprint matcher. The input images to Veri-Finger in the three experiments are original fingerprints, rectified fingerprints by Senior and Bolle approach, and rec-tified fingerprints by the proposed algorithms, respectively. No impostor matches were conducted because the matching score of VeriFinger is linked to the false accept rate (FAR). FVC2006 DB2_A was used to examine whether distortion rectification may have negative impact on matching accuracy in situations where distorted fingerprints are absent or scarce. The distorted subset of FVC2004 DB1 consists of 89 distorted fingerprints and mated normal fingerprints. It was separately tested in order to clearly evaluate the contribution of distortion rectification to matching distorted fingerprints alone. The ROC curves on the four databases are shown in

Fig. 14. From Fig. 14, we can clearly see that:

- 1) On all the four databases, Senior and Bolle algorithm actually reduces the matching accuracy;
- 2) On the databases containing many distorted fingerprints (FVC2004 DB1 and Tsinghua DF database), the proposed algorithm significantly improves the matching accuracy;
- 3) On the database without severely distorted fingerprints (FVC2006 DB2_A), the proposed algorithm has no negative impact.

Five examples from FVC2004 DB1 and Tsinghua DF database are given in Fig. 15 to compare the rectified results and matching performance of the three cases (no rectification, rectified by Senior and Bolle approach, and rectified by the proposed approach). In order to further evaluate the proposed rectification algorithm, we conducted a matching experiment on NIST

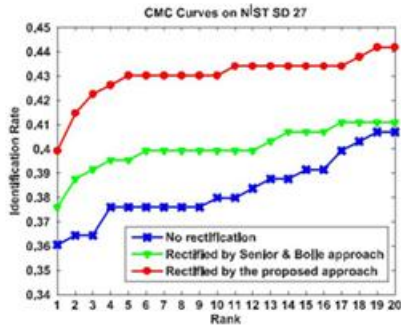


Fig. 16. The CMC curves of three matching experiments on NIST SD27: Original latent fingerprints (no rectification), latent fingerprints rectified by Senior and Bolle approach [28], and latent fingerprints rectified by the proposed approach.

SD27 latent database which contains some distorted latent fingerprints. VeriFinger was used as the fingerprint matcher. The cumulative match characteristic (CMC) curve is commonly used to report latent matching accuracy. To make the experiment more realistic, we use all 27,000 file fingerprints in the NIST SD14 database as the background database. Due to the complex background of latent fingerprints, the ridge.

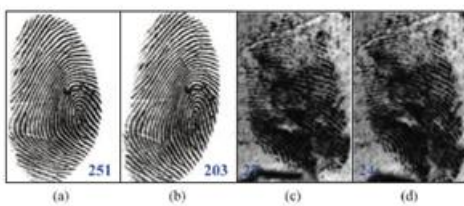


Fig. 18. Two examples of unsuccessful rectification due to non-frontal pose and low image quality. (a) Query fingerprint with non-frontal pose, and (b) and (a) rectified by the proposed algorithm; (c) query fingerprint in NIST SD27 with low image quality, and (d) and (c) rectified by the proposed algorithm. The matching scores with corresponding gallery finger-prints are overlaid.

Orientation map and period map extracted from the original image are not reliable.

So we use the features extracted from the enhanced fingerprints by the algorithm in [15] instead. Because of the small area of many latents, the distortion detection result is not reliable. Thus we apply the rectification algorithm to all latent fingerprints. Then we use a max rule to fuse the two matching scores: one from original fingerprint and the other from rectified fingerprint. The CMC curves on NIST SD27 shown in Fig. 16 correspond to the following three cases: no rectification, latent finger-prints rectified by Senior and Bolle approach, and latent.

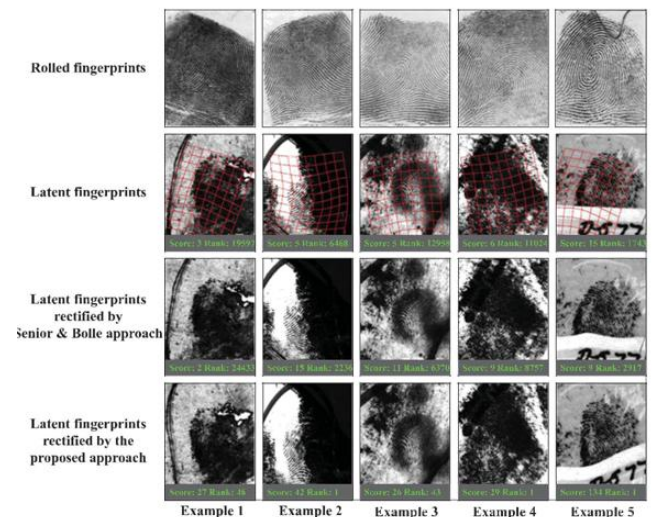


Fig. 17. Genuine match scores and ranks of original latent fingerprints and latent fingerprints rectified by two different approaches for five examples from NIST SD27.

The red transformation grids estimated by the proposed approach are overlaid on the original latent fingerprints to visualize the distortion. The proposed approach significantly improves the rank of corresponding rolled fingerprints.

TABLE 3
Statistics of Rectification Error

Database	Normal fingerprints (NError/Total)		Distorted fingerprints (NError/Total)	
	False positive	False negative	Low quality	Small area Non-frontal pose
Distorted subset of FVC 2004 DB1	0/89	7/89	5/89	0/89
Tsinghua DF	10/120	4/120	0/120	5/120

TABLE 4
Speed of the Proposed Distortion Detection and Rectification Algorithms

Algorithm	FVC2004 DB1		Tsinghua DF		NIST SD27	
	Time (sec)	Percentage	Time (sec)	Percentage	Time (sec)	Percentage
Detection with center point	1.2	89.43%	1.4	86.25%	-	-
Detection without center point	15.3	10.57%	16.8	1.77%	-	-
Rectification with center point	43.9	86.07%	64.5	97.02%	65.3	73.97%
Rectification without center point	67.1	13.91%	66.3	2.33%	67.5	24.03%

Fingerprints rectified by the proposed approach. From Fig. 16, we can see that both rectification algorithms can improve the recognition rate and the proposed algorithm performs better. Senior and Bolle approach also helps improve matching accuracy here because of the max fusion rule. Five examples from NIST SD27 are given in Fig. 17 to compare the rectified results by two algorithms. Although the genuine match scores of most distorted fingerprints are improved after rectification, there are some examples whose matching scores dropped after rectification. Unsuccessful rectification can be classified into two categories: (1) a normal fingerprint is incorrectly detected as a distorted one and then undergoes the rectification process, and (2) the rectification for a distorted fingerprint is incorrect. False positive of distortion detection is discussed in Section 5.1. The main causes for unsuccessfully rectified distorted fingerprints are non-frontal pose of finger, low image quality and small area. In these cases, there is no sufficient information for correctly estimating the distortion field. Such two examples are given in Fig. 18. We have examined all the matching pairs with reduced scores on the distorted subset of FVC 2004 DB1 and Tsing-hua DF database and has categorized the cause of error. The results are shown in Table 3. For a matching pair, if the normal fingerprint is a false positive, the cause is set as false

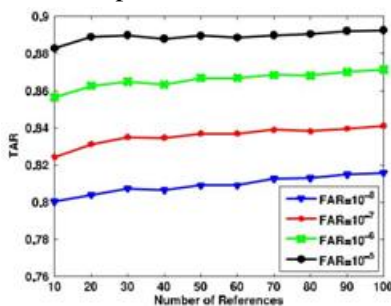


Fig. 19. The impact of the number of reference fingerprints on matching accuracy on the whole FVC2004 DB1.

Positive; otherwise, the distorted one is analyzed and the cause is set as low image quality, small finger area, and/or non-frontal pose of finger.

5.3 Impact of the Number of Reference Fingerprints:

The number of reference fingerprints used in distortion rectification is an important parameter. Fig. 19 shows the impact of the number of reference fingerprints on matching accuracy on FVC2004 DB1. As we can see from this figure, a larger number of reference fingerprints lead to higher matching accuracy. But a larger number of reference fingerprints also mean longer process time. In the experiments described in Section 5.2, we use 100 reference fingerprints to generate 12,100 distorted reference fingerprints. The average times of the proposed distortion detection and rectification algorithm on a PC with 2.50 GHz CPU are reported in Table 4. The percentages of fingerprints with/without center point are also reported in Table 4.

6 CONCLUSION:

False non-match rates of fingerprint matchers are very high in the case of severely distorted fingerprints. This generates a security hole in automatic fingerprint recognition systems which can be utilized by criminals and terrorists. For this reason, it is necessary to develop a fingerprint distortion detection and rectification algorithms to fill the hole. This paper described a novel distorted fingerprint detection and rectification algorithm. For distortion detection, the registered ridge orientation map and period map of a fingerprint are used as the feature vector and a SVM classifier is trained to classify the input fingerprint as distorted or normal. For distortion rectification (or equivalently distortion field estimation), a nearest neighbor regression approach is used to predict the distortion field from the input distorted fingerprint and then the inverse of the distortion field is used to transform the distorted fingerprint into a normal one. The experimental results on FVC2004 DB1, Tsinghua DF database, and NIST SD27 database showed that the proposed algorithm can improve recognition rate of distorted fingerprints evidently. A major limitation of the current approach is efficiency.

Both detection and rectification steps can be significantly speeded up if a robust and accurate fingerprint registration algorithm can be developed. Another limitation is that the current approach does not support rolled fingerprints. It is difficult to collect many rolled fingerprints with various distortion types and meanwhile obtain accurate distortion fields for learning statistical distortion model. It is our ongoing work to address the above limitations.

ACKNOWLEDGMENTS:

This work was supported by the National Natural Science Foundation of China under Grants 61225008, 61373074, and 61020106004, the National Basic Research Program of China under Grant 2014CB349304, the Ministry of Education of China under Grant 20120002110033, and the Tsinghua University Initiative Scientific Research Program.

REFERENCES:

- [1] X. Si, J. Feng, and J. Zhou, "Detecting fingerprint distortion from a single image," in Proc. IEEE Int. Workshop Inf. Forensics Security, 2012, pp. 1–6.
- [2] D. Maltoni, D. Maio, A. K. Jain, and S. Prabhakar, Handbook of Fingerprint Recognition, 2nd ed. Berlin, Germany: Springer-Verlag, 2009.
- [3] FVC2006: The fourth international fingerprint verification competition. (2006). [Online]. Available: <http://bias.csr.unibo.it/fvc2006/>
- [4] V. N. Dvornychenko, and M. D. Garris, "Summary of NIST latent fingerprint testing workshop," Nat. Inst. Standards Technol., Gaithersburg, MD, USA, Tech. Rep. NISTIR 7377, Nov. 2006.
- [5] Neurotechnology Inc., VeriFinger. (2009). [Online]. Available: <http://www.neurotechnology.com>
- [6] L. M. Wein and M. Baveja, "Using fingerprint image quality to improve the identification performance of the U.S. visitor and immigrant status

indicator technology program," Proc. Nat. Acad. Sci. USA, vol. 102, no. 21, pp. 7772–7775, 2005.

[7] S. Yoon, J. Feng, and A. K. Jain, "Altered fingerprints: Analysis and detection," IEEE Trans. Pattern Anal. Mach. Intell., vol. 34, no. 3, pp. 451–464, Mar. 2012.

[8] E. Tabassi, C. Wilson, and C. Watson, "Fingerprint image quality," Nat. Inst. Standards Technol., Gaithersburg, MD, USA, Tech. Rep. NISTIR 7151, Aug. 2004.

[9] F. Alonso-Fernandez, J. Fierrez-Aguilar, J. Ortega-Garcia, J. Gonzalez-Rodriguez, H. Fronthaler, K. Kollreider, and J. Bigun, "A comparative study of fingerprint image-quality estimation methods," IEEE Trans. Inf. Forensics Security, vol. 2, no. 4, pp. 734–743, Dec. 2007.

[10] J. Fierrez-Aguilar, Y. Chen, J. Ortega-Garcia, and A. K. Jain, "Incorporating image quality in multi-algorithm fingerprint verification," in Proc. Int. Conf. Biometrics, 2006, pp. 213–220.

[11] L. Hong, Y. Wan, and A. K. Jain, "Fingerprint image enhancement: Algorithm and performance evaluation," IEEE Trans. Pattern Anal. Mach. Intell., vol. 20, no. 8, pp. 777–789, Aug. 1998.

[12] S. Chikkerur, A. N. Cartwright, and V. Govindaraju, "Fingerprint enhancement using STFT analysis," Pattern Recognit., vol. 40, no. 1, pp. 198–211, 2007.

[13] F. Turrone, R. Cappelli, and D. Maltoni, "Fingerprint enhancement using contextual iterative filtering," in Proc. Int. Conf. Biometrics, 2012, pp. 152–157.

[14] J. Feng, J. Zhou, and A. K. Jain, "Orientation field estimation for latent fingerprint enhancement," IEEE Trans. Pattern Anal. Mach. Intell., vol. 35, no. 4, pp. 925–940, Apr. 2013.



[15] X. Yang, J. Feng, and J. Zhou, "Localized dictionaries based orientation field estimation for latent fingerprints," *IEEE Trans. Pattern Anal. Mach. Intell.*, vol. 36, no. 5, pp. 955–969, May 2014.

[16] R. M. Bolle, R. S. Germain, R. L. Garwin, J. L. Levine, S. U. Pan-kanti, N. K. Ratha, and M. A. Schappert, "System and method for distortion control in live-scan inkless fingerprint images," U.S. Patent No. 6 064 753, May 16, 2000.